Journal of Colloid and Interface Science 640 (2023) 220–229

Contents lists available at ScienceDirect

Journal of Colloid and Interface Science

journal homepage: www.elsevier.com/locate/jcis

Probing the effect of the capping polyelectrolyte on the internal structure of Layer-by-Layer decorated nanoliposomes

Ana Mateos-Maroto [a,1,*], José E. F. Rubio [b], Sylvain Prévost [c], Armando Maestro [d,e], Ramón G. Rubio [a], Francisco Ortega [a,f], Eduardo Guzmán [a,f,*]

[a] Departamento de Química Física, Facultad de Ciencias Químicas, Universidad Complutense de Madrid, Ciudad Universitaria s/n, 28040-Madrid, Spain
[b] Centro de Espectroscopía y Correlación, Universidad Complutense de Madrid, Ciudad Universitaria s/n, 28040-Madrid, Spain
[c] Institut Laue-Langevin, 71 Avenue des Martyrs, CEDEX 9, 38042 Grenoble, France
[d] Centro de Física de Materiales (CSIC, UPV/EHU)-Materials Physics Center MPC, Paseo Manuel de Lardizabal 5, 20018-San, Sebastián, Spain
[e] IKERBASQUE—Basque Foundation for Science, Plaza Euskadi 5, 48009-Bilbao, Spain
[f] Unidad de Materia Condensada. Instituto Pluridisciplinar, Universidad Complutense de Madrid, Paseo Juan XXIII 1, 28040 Madrid, Spain

GRAPHICAL ABSTRACT

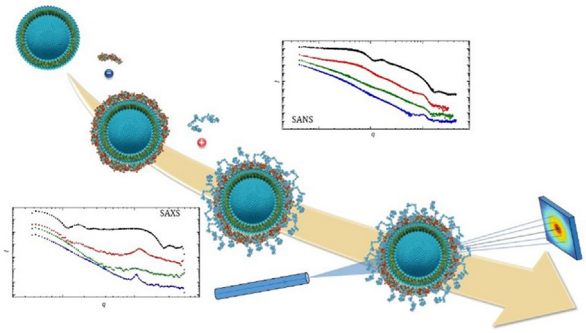

ARTICLE INFO

Article history:
Received 11 November 2022
Revised 2 February 2023
Accepted 15 February 2023
Available online 18 February 2023

Keywords:
Capsules
Layer-by-layer
Liposomes
Polyelectrolyte multilayer
Scattering
Structure

ABSTRACT

Hypothesis: The internal organization of polyelectrolyte layers deposited on colloidal templates plays a very important role for the potential applications of these systems as capsules for drug delivery purposes.
Experiments: The mutual arrangement of oppositely charged polyelectrolyte layers upon their deposition on positively charged liposomes has been studied by combining up three different scattering techniques and Electronic Spin Resonance, which has provided information about the inter-layer interactions and their effect on the final structure of the capsules.
Findings: The sequential deposition of oppositely charged polyelectrolytes on the external leaflet of positively charged liposomes allows modulating the organization of the obtained supramolecular structures, impacting the packing and rigidity of the obtained capsules due to the change of the ionic cross-linking of the multi-layered film as a result of the specific charge of the last deposited layer. The possibility to modulate the properties of the LbL capsules by tuning the characteristics of the last deposited layers offers a very interesting route for the design of materials for encapsulation purposes with their properties controlled almost at will by changing the number of deposited layers and their chemistry.

* Corresponding authors.
E-mail addresses: mateosa@mpip-mainz.mpg.de (A. Mateos-Maroto), eduardogs@quim.ucm.es (E. Guzmán).
[1] Current Address: Max Planck Institute for Polymer Research, Ackermannweg 10, 55128 Mainz, Germany.

https://doi.org/10.1016/j.jcis.2023.02.086
0021-9797/

1. Introduction

The use of the Layer-by-Layer (LbL) method for the fabrication of supramolecular capsules by the alternate assembly of layers of polyelectrolytes bearing oppositely charges on soft colloids (emulsion droplets, liposomes, and vesicles) has gained importance in recent years, taking advantage of the modularity and versatility of the LbL method for the fabrication of supramolecular systems incorporating well-defined environments for drug inclusion [1–6]. However, the exploitation of this approach in the rational design of capsules with true applications requires a deep understanding of different physicochemical aspects, e.g., permeability, mechanical resistance or surface charge, and structural aspects of the assembled system, which many times are not easily accessible [7]. In particular, there is an important lack of knowledge related to the packing and organization of the layers upon their deposition on soft colloidal templates, e.g., liposomes or liquid droplets, which are becoming a very interesting alternative for the design of different drug delivery systems and devices for theranostics [8–12].

The main advantage of the use of soft colloidal objects as templates for the fabrication of capsules by the LbL method arises from the fact that most of these colloidal objects present an organized environment for including the molecules to be encapsulated [4,5], and hence the final capsule does not require any chemical or physical treatment after their fabrication for obtaining a hollow capsule as happened when typical colloidal particles are used [13–16]. Therefore, LbL capsules on soft colloidal templates present an elegant combination of the main characteristics of the templates with the ability for modulating the physicochemical properties of the template provided by the assembly of a LbL film, making these systems very promising tools in different biomedical fields [4,17,18].

Considering the potential applications envisaged for multilayered capsules on soft colloidal templates it is necessary to deepen on their assembly by evaluating their thickness and internal structure. These aspects have been extensively studied for polyelectrolyte films supported on flat surfaces [19–23]. However, the knowledge about the layer organization on colloidal templates, and in particular on soft colloidal templates has been less explored, and many questions remain open [24–26]. A suitable answer to such questions is essential for gaining knowledge for optimizing the properties of the capsules, and in particular, the wall properties for fabricating capsules with stability, thickness, and permeability tuned at will.

The use of small-angle neutron, SANS and X-ray ray scattering, SAXS, respectively, emerges as very powerful tools for a spatial characterization of the internal structure of polyelectrolyte capsules in the nanometric scale. This characterization is difficult by other techniques such electronic or atomic force microscopies that require a pre-treatment of the samples and/or their attachment to substrates. This makes impossible to obtain high-resolution spatial information on soft colloids in their native state. In fact, electronic microscopy experiments require, in most cases, the study of samples in absence of solvent and/or under high vacuum conditions which can force the aggregation, deformation or even the rupture of soft colloids. Moreover, the necessity of supporting the samples for its visualization in the above mentioned microscopy techniques can also contribute to obtain structural information about the capsules that is not provides a true representation of the system under preparation, storage or application conditions. Furthermore, SANS and SAXS provide information even on the wall thickness which is not easily accessible by other techniques, such as dynamic light scattering (DLS) or cryogenic transmission electronic microscopy (cryo-TEM) [27]. SANS and SAXS provide important information on the density profiles along with the multilayer structure, which can be used for deepening on the characterization of the organization of the polyelectrolyte layers in relation to the template. The combination of scattering results with data obtained by using other techniques, e.g., Electron Spin Resonance (ESR), can contribute obtaining a realistic picture of the internal structure of polyelectrolyte films deposited on soft colloidal templates [27].

This work explores, by combining up to three different scattering techniques (SANS, SAXS and DLS) and ESR, the assembly of polyelectrolyte multilayers from two different pairs, namely PSS/PAH onto positively charged liposomes, (PSS being poly(4 styrene sulfonate of sodium) and PAH being poly(allyalmine hydrochloride)) and PSS/PDADMAC (with PDADMAC being poly(diallyldimethylammonium chloride)), to evaluate the mutual arrangement of polyelectrolyte layers and their impact on the final structure of the obtained capsules.

2. Materials and methods

2.1. Chemicals

1,2-dioleoyl-*sn*-*glycero*-3-phosphocholine (DOPC) with a purity higher than 99 % was purchased from Avanti Polar Lipids, Inc. (Alabaster, AL, USA) and stored at −20 °C. Dimethyldioctadecylammonium bromide (DODAB) was supplied by Sigma-Aldrich (Saint Louis, MO, USA) and stored a 25 °C. The anionic polyelectrolyte poly(4 styrene sulfonate of sodium) (PSS) with a molecular weight of 70 kDa and the cationic ones poly(allylamine hydrochloride) (PAH) with a molecular weight of 17 kDa and poly(diallyldimethylammonium chloride) (PDADMAC) with molecular weight in the range 100–200 kDa, were used for the fabrication of the polyelectrolyte multilayers. The three polyelectrolytes were supplied by Sigma Aldrich (Saint Louis, MO, USA). For Electron Spin Resonance measurements, the spin-labeled phospholipid, 4-Palmitamido-2,2,6,6-tetramethylpiperidine-1 oxyl (*N*-TEMPO) supplied by Sigma Aldrich (Saint Louis, MO, USA) was included in the lipid membrane. All chemicals were used as received without further purification. The ionic strength of the solutions was fixed using NaCl with purity higher than 99.99 % and purchased from Sigma Aldrich (Saint Louis, MO, USA).

All the solutions were prepared by weighting with a precision of ± 1 mg. The used water for cleaning and preparing the solutions was of Milli-Q quality obtained by a multi-cartridge purification system aquaMAX^{TM}-Ultra 370 Series (Young Lin Instrument, Co., Anyang, South Korea), with its resistivity being higher than 18 MΩ cm and its total organic content lower than 6 ppm. Solutions for SANS and SAXS experiments were prepared using deuterium oxide with purity of 99.9 % evaluated as the percentage of deuterium atoms, supplied by Sigma Aldrich (Saint Louis, MO, USA).

2.2. Preparation of the liposomes

The preparation of liposomes was performed by extrusion, which is a multistep procedure that allows obtaining dispersions of monodisperse unilamellar liposomes [28]. This procedure may be summarized as follows. First, the required amounts of lipids (10 mg) for preparing a final solution of concentration 1 mg/mL are weighted and poured in a 10 mL flask. Then, chloroform (10 mL) is added to prepare the solutions containing lipid mixtures with the desired weight fraction of each component (70 % of DOPC and 30 % of DODAB). The lipid solution is then homogenized by vortexing during 2 min. Afterwards, the organic solvent was evaporated under a nitrogen stream to obtain a dry lipid film, and left overnight at −20 °C to ensure its complete stabilization. The lipid film was later rehydrated by adding 10 mL of an aqueous solution

containing NaCl (10 mM). During the rehydration process, it was necessary to heat the lipid mixtures above the melting temperature of the lipids and to homogenize the dispersion by vigorous vortexing. The rehydration process yields a suspension of tiny pieces of membranes and multilamellar vesicles, which is subjected to an extrusion process using a Thermobarrel Lipex Extruder from Northern Lipids (Burnaby, Canada) for obtaining small unilamellar vesicles (SUVs). The extrusion process involved passing an odd number of times (minimum 11) the above-mentioned suspensions through polycarbonate membranes of controlled pore size (Nucleopore® Track-Etched Membranes, Avanti Polar Lipids, Inc., Alabaster, AL, USA) to obtain a dispersion of monodisperse liposomes with an average diameter close to the pore size of the used membranes. The optimization of the preparation of liposomes with average diameters of 100, 80, or 50 nm, requires to perform a progressive reduction of the liposome sizes by passing the dispersion through membranes with a pore diameter of 400 and 200 nm, before performing the final extrusion with membranes having a pore size similar to the desired diameter of the final unilamellar liposomes. The progress of the extrusion process was checked by evaluating the hydrodynamic radius of the liposomes obtained by dynamic light scattering (DLS) after each five extrusion steps.

2.3. LbL assembly

The liposomes obtained were used as a template for the LbL assembly of polyelectrolyte layers, following the methodology described in our previous publication [27]. For this purpose, a 5-fold dilution of the liposome suspension (from 1 mg/mL to 0.2 mg/mL) was required before adding the polyelectrolyte layers for avoiding flocculation or aggregation events, which in turn can result in the destabilization of the suspension. To form the first polymeric layer, the appropriate amount of the anionic polyelectrolyte (concentration 1 mg/mL) needed to reach the charge inversion according to electrophoretic mobility measurements (see our previous publication [27] for data and detailed discussion of the electrophoretic mobility results) is added to the liposome suspension. Then, the mixture of the liposomes and polyelectrolyte is homogenised by vortexing for 5 min, allowing the formation of the first polyelectrolyte layer on the liposome surface. Afterwards, an excess of cationic polyelectrolyte solution (concentration 1 mg/mL) was added to the above mixture. This leads to the formation of a second polyelectrolyte layer, whereas the non-adsorbed polycation leads to the formation of inter-polyelectrolyte complexes (IPECs) by electrostatic interactions with the chains of polyanion remaining in the aqueous phase after the deposition of the first layer. These IPECs precipitate, which enables their separation from the dispersion of coated liposomes by centrifugation at 10000 rpm (14200 g). The sequential addition of polyelectrolytes followed by the separation of IPECs was repeated until the desired number of deposited layers was attained. The effective adsorption of each layer was checked by DLS and zeta potential measurements (the corresponding zeta potential variation with the number of coating layers, N, is shown in Figure S1 in Supporting Material).

2.4. Methods

Dynamic Light Scattering (DLS) measurements for evaluating the hydrodynamic radius, R_H, of liposomes coated with polyelectrolyte multilayers were performed using a Malvern Zetasizer Nano ZS instrument (Malvern Instruments, ltd., Malvern, United Kingdom) [29,30]. The DLS measurements were performed at 25 °C in quasi-backscattering configuration (scattering angle, θ = 173°) using the red line of a He-Ne laser working at a wavelength λ = 632.8 nm. Before each measurement, the samples were filtered in a cleanroom using Nylon filters of 0.45 μm of diameter (Millex®, Merck-Millipore, Burlington, MA, USA) to remove dust particles, and transfer them to the measurement cells.

The zeta potential of the coated liposomes, ζ, can be inferred from measurements of electrophoretic mobility, u_e, obtained by Laser Doppler velocimetry performed using a Zetasizer Nano ZS (Malvern Instrument, ltd., Malvern, United Kingdom). The measured values of μ_e were transformed into ζ values using Henry's relationship, assuming that the particles fulfill Smoluchowski's limit [31]. The accuracy in the determination of the zeta potential was better than ± 5 mV, which is important for the evaluation of the isoelectric point.

Electron Spin Resonance spectra were obtained on a Bruker EMX spectrometer (Bruker, Billerica, MA, USA) that works in continuous wave and uses the X-band resonator on the microwave region (~9.5 GHz). ESR spectra were recorded in the temperature range 15–60 °C.

Small Angle Neutron Scattering (SANS) experiments were performed using the lowest momentum transfer and lowest background small-angle neutron scattering instrument of the D11 beamline at the Institute Laue-Langevin (ILL, Grenoble, France). Samples were measured using Hellma quartz 120-QS cells of 1 mm pathway over a q-range of 2.5 10^{-3} to 0.6 $Å^{-1}$ at a single wavelength of 6.0 Å (FWHM 10 %) with 3 sample-to-detector distances of 1.5 m, 5.6 and 17.6 m. Absolute scale was obtained from the flux using the attenuated direct beam. Data correction was performed using Grasp, accounting for transmission, flat field, detector noise (measurement of boron carbide absorber); the contribution from the solvent was subtracted. The corresponding neutron scattering profiles were recorded as a function of the number of adsorbed layers.

Small Angle X-ray Scattering experiments were carried out at the BioSAXS BM29 beamline at The European Synchrotron Radiation Facility (ESRF, Grenoble, France). In both techniques, the wavevector, q, is defined as

$$q = \frac{4\pi}{\lambda_i} sen\theta \tag{1}$$

where λ_i is the wavelength of the incident beam in vacuum and θ the scattering angle.

3. Results and discussion

3.1. Structural characterization of bare liposomes

SANS and SAXS experiments were performed to study the geometry of the polyelectrolyte capsules as well as the internal organization of the deposited layer and how these characteristics are modified by the adsorption of the consecutive polymer layers. For this purpose, it is necessary to first characterize the structure of the liposomes used as templates for the LbL deposition, i.e., DOPC: DODAB liposomes with 70:30 compositional ratio. Fig. 1 shows the reflectivity profiles obtained by SANS and SAXS for liposomes with three different sizes defined by the radius of the membranes used for their preparation by extrusion ($R_{nominal}$ = 25, 40 and 50 nm).

Assuming that liposomes are hollow spheres, it is possible to describe the experimental SANS profiles by using a form factor, $P(q)$, described by

$$P(q) = \frac{\phi}{V_{shell}} \left[\frac{3V_{core}(\rho_{dis} - \rho_{shell}) j_1(qR_{core})}{qR_{core}} + \frac{3V_t(\rho_{shell} - \rho_{dis}) j_1(qR_{core})}{qR_t} \right]^2 \tag{2}$$

where ϕ and V_{shell} are the particle volume fraction and the lipid bilayer volume, respectively, V_{core} is de liposome inner volume, V_t the total volume, R_{core} and R_t the liposome inner radius and total radius, ρ_{dis} and ρ_{shell} are the scattering length densities of the sol-

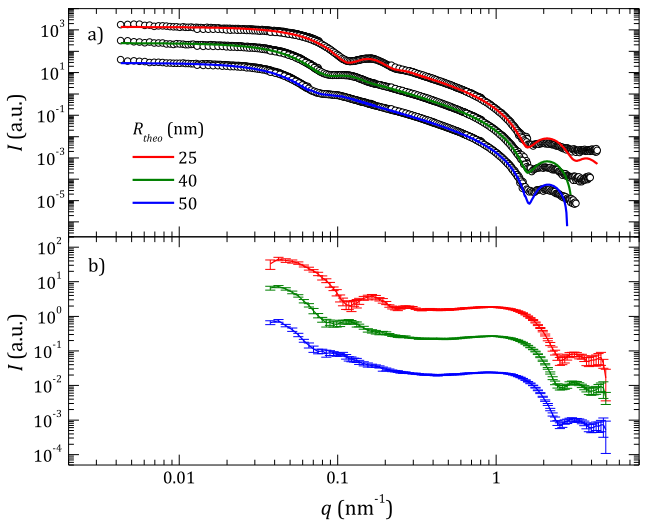

Fig. 1. A) sans and b) saxs scattering profiles of liposomes of different nominal diameter with a composition 70:30 DOPC:DODAB. The solid lines correspond to the modelled scattering profiles.

vent and the bilayer, and j_1 is the spherical Bessel function $j_1 = (sen(x) - \cos(x))/x^2$ [32]. The experimental SANS profiles present a decay of the reflected intensity as the wavevector increases, with two peaks that are characteristic of different structural features of the system. The first peak, in the range of wavevectors 0.10–0.15 nm^{-1}, provides information related to the size of the liposome, whereas the second one appears at higher values of q (around 2 nm^{-1}), and provides information related to the thickness of the membrane, i.e., the thickness of the hydrophobic chains of the lipid molecules [33]. On one side, the intensity of the first peak on the SANS reflectivity profile decreases with the increase of the liposome size, which is ascribed to the decrease of the resolution of SANS as the size of the scatters increases [34]. On the other side, the peak corresponding to the membrane thickness appears well-defined independently of the liposome size, having a value of about 4 nm as reported in Table 1. This table reports the characteristic values corresponding to the radius of the inner core of the liposome (R_{core}), the thickness of the lipid bilayer ($t_{bilayer}$) and the total radius of the liposomes ($R_{TOTAL} = R_{core} + t_{bilayer}$). These values were obtained from the analysis of the experimental reflectivity profiles obtained by SANS using a hollow sphere model. For the sake of comparison, the hydrodynamic diameter values obtained by DLS measurements are also reported in Table 1.

It is worth mentioning that the hydrodynamic radii obtained by DLS are slightly higher than those obtained by SANS in agreement with the results reported in the literature for other liposomes of phosphatidylcholines [35]. This is explained considering that both techniques provide physically different radii: SANS experiments give information about the true dimension of the scatters, whereas DLS provides information on a radius that includes both the liposomes and the hydration layer [36].

SAXS profiles agree with those obtained by SANS [37]. The former profiles also present two characteristic peaks. The first peak, appearing in the wavevector range 0.10–0.16 nm^{-1}, is related to the size of the liposome, whereas the second one appearing around 3.1 nm^{-1} provides information about the thickness of the lipid membrane. Furthermore, the absence of Bragg peaks is an indication of the unilamellar character of the liposomes[38].

Fig. 2 reports the pair distributions functions $p(r)$, obtained from the inverse Fourier transformation of the SAXS curves, of liposomes of 80 and 50 nm in diameter. Unfortunately, liposomes with sizes of 100 nm present higher polydispersity, which makes very difficult to obtain well-defined $p(r)$ profiles. The pair distribution functions obtained for liposomes of the two sizes are in agreement with the above-discussed structure of a hollow sphere, where the maximum of the distribution appears to have a characteristic size above $D_{max}/2$[39], with D_{max} being the distance where $p(r) = 0$, providing an idea about the maximum diameter of the liposomes.

From the analysis of the $p(r)$ profiles by deconvolution, using Gaussian profiles, it is possible to obtain three characteristic lengths (values reported in Table 1), as is depicted in the inset in Fig. 2: (i) the local maximum at low distances corresponds to the bilayer thickness, t_b, (ii) the liposome diameter is given by the distribution maximum d, and (iii) the shoulder at medium distances is related with radius, R. It should be noted that the broad character of the $p(r)$ profile for liposomes of 80 nm (see Fig. 2a) confirms that such liposomes present a relatively high polydispersity.

Moreover, the analysis of the $p(r)$ profiles allows one to a fast elucidation of the morphology of the studied particles, providing a preliminary evaluation of some structural parameters. For this reason, a Guinier analysis was performed for the low q region of the SAXS curves, thus from the ln $I(q)$ vs q^2 plots it is possible to obtain information on the radius of gyration, R_g, of each sample. The corresponding analysis and obtained data are shown in Figure S2 of Supporting Information and Table 1, respectively. It should be stressed that the results for the size of the liposomes and the bilayer thickness obtained for the different techniques are in good agreement.

The use of three different scattering techniques (DLS, SANS and SAXS) has made it possible to perform a deep and reliable structural characterization of liposome dispersions, which is essential to ensure the good quality of the starting material for fabricating LbL decorated liposomes. Thus, SANS and SAXS have provided complementary information related to the sample, as X-ray scattering is more sensitive to the polar heads of the lipid bilayer, whereas neutron scattering is to the hydrophobic chains. On the other side, DLS has provided important dynamic information to complement the structural findings obtained by using the other two techniques.

3.2. Lateral organization of lipids in the liposome bilayer

The fluidity of the lipid bilayers may impact decisively on the deposition process of polyelectrolyte layers on the liposome surface because membrane fluidity can influence the specific conformation of the polyelectrolyte chains directly associated with the liposomes, regulating the possible insertion of polyelectrolyte chains within the external leaflet of the liposomes [40]. Therefore, it is important to perform a preliminary evaluation of the membrane fluidity for liposomes used as a template by Electron Spin Resonance (ESR) experiments [41]. Firstly, the fluidity of the membrane of single lipids, i.e., DOPC (zwitterionic liposomes) and DODAB (cationic liposomes) were analyzed at different temperatures. Fig. 3a and 3b report the ESR spectra obtained for DODAB and DOPC liposomes.

Independently of the liposome composition and the considered temperature, the spectra are highly symmetric, at least for the two first peaks, whereas the third peak presents a decrease in its average intensity. This indicates that for the studied liposomes, the labeled lipid is confined within a mostly fluid environment [42]. In the particular case of DODAB liposomes, this behaviour emerges from temperatures below the gel-ordered liquid phase transition (around 45 °C) [43], which clearly indicates that such phase transition does not affect significantly the membrane dynamics for pure DODAB liposomes. Furthermore, the spectra for DODAB liposomes show that the value of the magnetic field corresponding to the maximum intensity drops for temperatures in the range 40 °C-45 °C, i.e. around the phase transition. This may indicate a local

Table 1
Data obtained by DLS, SANS and SAXS of liposomes of different nominal diameters with composition 70:30 DOPC:DODAB. In SANS data, R_{TOTAL} is the sum of R_{core} and $R_{bilayer}$. In this table, *PD* appears as the polydispersity obtained as the standard deviation of the corresponding R_{core} and $t_{bilayer}$ values.

	DLS		SANS					SAXS				
R (nm)	R_H (nm)	*PdI*	R_{core} (nm)	*PD*	$t_{bilayer}$ (nm)	*PD*	R_{TOTAL} (nm)	Rg (nm)	t_b (nm)	*R* (nm)	*d* (nm)	D_{max} (nm)
50	55.6 ± 0.2	0.08 ± 0.02	32.59 ± 0.02	0.32	3.97 ± 0.01	0.07	36.56 ± 0.03	44 ± 2	–	–	–	–
40	45.8 ± 0.9	0.08 ± 0.02	30.92 ± 0.02	0.25	4.00 ± 0.01	0.08	34.92 ± 0.03	39.0 ± 0.3	5.2 ± 0.8	30 ± 3	61 ± 2	96.9
25	35.3 ± 0.3	0.08 ± 0.02	23.72 ± 0.01	0.18	4.01 ± 0.01	0.08	27.72 ± 0.02	29.7 ± 0.7	4.3 ± 0.2	23 ± 1	45 ± 1	64.4

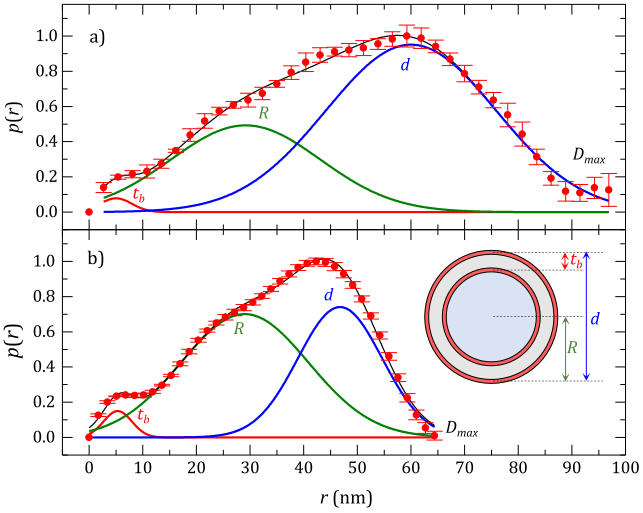

Fig. 2. Pair distribution function $p(r)$ for liposomes with composition 70:30 DOPC: DODAB, and two different nominal diameters: a) 80 nm and b) 50 nm. The symbols show the typical profile corresponding to a hollow sphere, and the lines represent the profiles corresponding to the peaks for characteristics features of the liposome structure obtained from the deconvolution of the experimental profile. The inserted scheme in panel b shows the best model accounting for the structure of the liposome and its different characteristic features.

change on the environment of the labelled molecules as result of the phase transition (see Fig. 3a and Figure S3 in Supporting Material). On the contrary, there are no evidences of any significant change of the value of the magnetic field corresponding to the maximum intensity with temperature for DOPC liposomes. This may be understood considering the absence of phase transitions for the DOPC liposomes in the range of temperatures explored, i.e., experiments were performed above the characteristic phase transition temperature of the DOPC (around – 20 °C) [44], and hence the labelled lipids are always in an environment with similar fluidity. The effect of the transition temperature in DODAB liposomes is also evidenced from the temperature dependence of the relaxation times, τ, obtained from the ESR spectra shown in Fig. 4, obtained by the following expression [45]

$$\tau(s) = 6,5 \cdot 10^{-10} \Delta H_0 [(h_0/h_{-1})^{1/2} - 1] \quad (2)$$

where ΔH_0 and h_0 are the width and height of the central peak, respectively, and h_{-1} the height of the third peak. For DODAB liposomes, the relaxation time drops for temperatures in the range 30–35 °C, which may be ascribed to a pre-ordering transition towards the formation of a phase of intermediate order, which acts as a precursor of the final ordered phase as was reported by Ji et al. [46]. Furthermore, the characteristic relaxation times for temperatures below 30 °C are higher, i.e., the relaxation is slower, for DODAB liposomes than for DOPC ones, which is an indication of the rigid environment of the labelled lipid in DODAB liposomes below the phase transition temperature. The restriction of the mobility of the labelled lipid within a rigid environment makes it necessary to increase the accumulation time required for obtaining resolved spectra, which justifies the error bars obtained for the τ values of DODAB liposomes below 30 °C. The situation changes with the increase of the temperature above 30 °C and the characteristic relaxation times for the labelled lipid in DODAB liposomes become comparable to those found for DOPC liposomes within the entire range of temperatures. This may be understood considering the higher mobility of the labelled lipid as a result of the fluid character of the membrane. It is should be stressed that for fluid phases the higher the temperature the lower the viscosity, which enhances the mobility of the lipids, with the relaxation times following an Arrhenius-like dependence, as is displayed for DOPC liposomes in Figure S4 (see Supporting Material).

In this work, the results are focused on the deposition of polyelectrolyte LbL multilayers on liposomes with a weight composition of 70 % DOPC and 30 %. The obtained ESR spectra for such liposomes at different temperatures are shown in Fig. 3c. The spectra are quite similar to those discussed above for liposomes of pure DOPC and DODAB, where the spin labelled lipid is confined in the bilayer under a mostly fluid environment. However, for liposomes of the mixture of DODAB and DOPC, no displacement is observed in the spectrum peaks with temperature. Furthermore, the relaxation times follow a similar dependence with the temperature than the one of liposomes containing only DOPC (see Fig. 4). This is reasonable considering that the DOPC is the main component of the liposomes considered.

The above discussion pointed out that the inclusion of DOPC molecules in the DODAB lamellae leads to a fluidification of the liposome membrane, as suggested by the decrease of the temperature associated with the phase transition. However, this is not enough to modify the membrane microviscosity, as evidenced by the similarities of the relaxation times for liposomes with different DOPC:DODAB ratio and those containing only DOPC. It should be stressed that the τ values obtained, and the profiles of the spectra appear rather similar to those reported in the literature for liposomes formed by phosphocholines [47].

3.3. Effect of the adsorption of polyelectrolyte layer on the lipid packing in the liposome bilayer: Ionic cross-linking

The polyelectrolyte adsorption on the liposomes is mainly governed by the direct electrostatic interactions between the polyelectrolyte chains and the surface charges on the liposomes, both bare and decorated with a certain number of layers, and hence it may be expected that this interaction could affect the membrane dynamics. This means that the ionic cross-linking between the external leaflet of the liposomes and the first polyelectrolyte layers, and between adjacent polyelectrolyte layers, may influence the microviscosity of the lipid membrane, and as matter of fact the in-plane mobility of lipids molecules [48]. To shed light on this aspect, ESR experiments at 50 °C were performed as a function of the number of adsorbed layers for different pairs, PSS/PAH and PSS/PDADMAC (see Fig. 5). It should be reminded that bare DODAB liposomes present an average positive charge, and the first layer deposited on their surface corresponds to the polyanion, i.e., PSS.

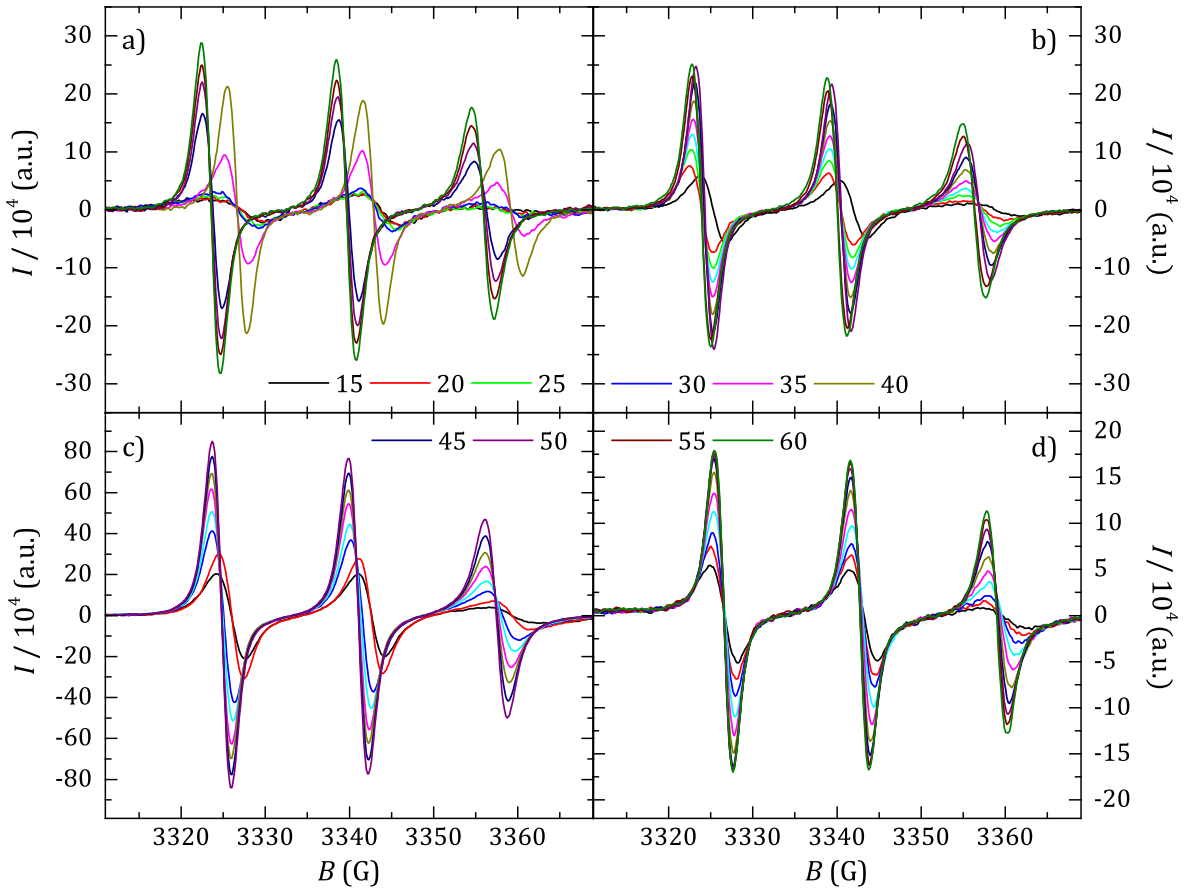

Fig. 3. Electron Spin Resonance spectra (intensity I vs magnetic field B) obtained in the range of 15 to 60 °C for liposomes with different composition: a) DODAB, b) DOPC, c) 70:30 DOPC:DODAB, and d) 30:70 DOPC:DODAB. The lines with different colours correspond to experiments performed at different temperatures.

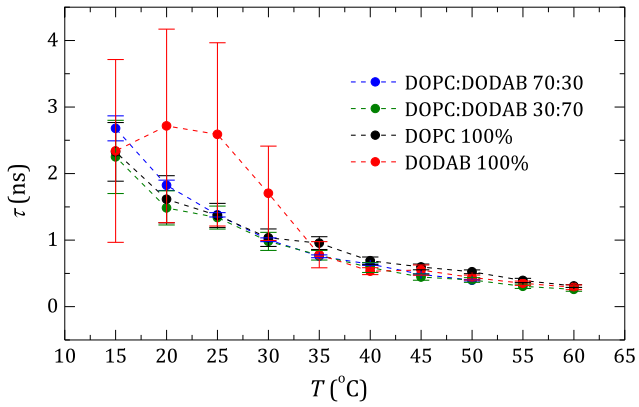

Fig. 4. Relaxation times, τ, obtained from the ESR profiles for liposomes with composition of 70:30 and 30:70 DOPC:DODAB, DOPC and DODAB.

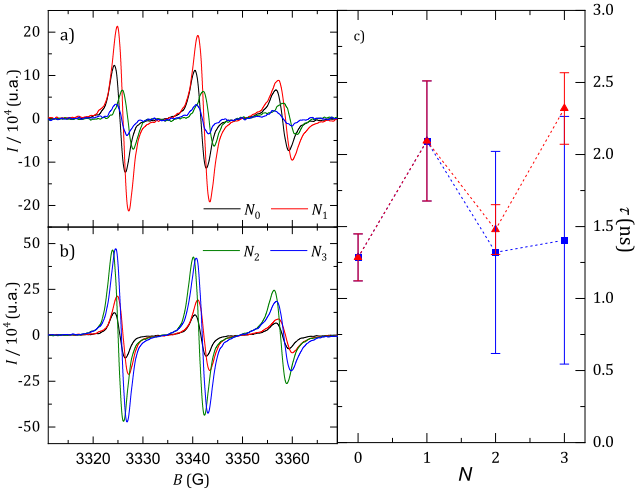

Fig. 5. ESR spectra (intensity I vs magnetic field B) registered at 50 °C corresponding to bare 70:30 DOPC:DODAB liposomes and coated with up to three polyelectrolyte layers (N_0: bare liposome, N_1: liposome + one polyelectrolyte layer, N_2: liposome + two polyelectrolyte layers and N_3: liposome + three polyelectrolyte layers). a) Liposomes decorated with layers of PSS/PAH pair, b) liposomes decorated with layers of PSS/PDADMAC pair and c) dependence of the relaxation times on the number of deposited layers, N. Blue squares correspond to PSS/PAH pair and red triangles to PSS/PDADMAC pair. (For interpretation of the references to colour in this figure legend, the reader is referred to the web version of this article.)

The results point out a clear displacement of the spectra maxima with the number of deposited layers, N, in all the samples. This indicates a modification of the lipid membrane dynamics as a result of the strong interaction with the adsorbed layers, in agreement with our previous findings [27]. Therefore, it may be reasonable to expect that direct interaction of the polyelectrolyte molecules of the first adsorbed layer, polyanion PSS with DODAB molecules of the external leaflet of the liposome may induce a strong ionic cross-linking between the lipid molecules and the first PSS layer, or even induce a change of the composition of the external and external layers of the membranes. Hence it may be expected that the adsorption of a polyanion layer directly on the liposome surface may change the microviscosity of the lipid bilayer, enhancing its lateral packing [49]. This is confirmed by

the results in Fig. 5c where the relaxation times, obtained from the analysis of the spectra for the studied systems as a function of the number of adsorbed polyelectrolyte layers are shown. The results evidence, independently of the polyelectrolyte pair used for decorating the liposomes, an odd–even effect on the relaxation time with the number of deposited layers, the relaxation times of liposomes coated with an odd number of layers being smaller than those with an even number of adsorbed layers. This may be understood considering the nature of the interactions between the lipids and the polyelectrolyte chains. Thus, it may be expected that the electrostatic interaction between the polyanion molecules, i.e., PSS chains, and the cationic surfactant, and in turn the ionic cross-linking, enhances the rigidity of the environment surrounding the molecules of the ESR labelled lipids. On the other side, the adsorption of the polycation on the surface of the polyanion-decorated liposomes results in the opposite effect. Thus, the electrostatic interaction between the adsorbing polycation molecules and the polyanion layer counteracts the attractive interactions between the first adsorbed layer with DODAB molecules in the external leaflet of the liposome, which in turn drives to the re-fluidification of the liposome membrane and the reduction of the relaxation times. These mechanisms of rigidification-fluidification of the liposomes as a consequence of the deposition of alternate layers with opposite charges should be propagated to the most external adsorbed layers, even though its impact on the membrane dynamics would be attenuated as the number of layers of the LbL film increases. This effect should be smaller for polyelectrolytes in which the charge compensation is of the extrinsic type.

3.4. Structure of polyelectrolyte decorated liposomes

As was above used for the structural characterization of bare liposomes, SANS and SAXS experiments were performed for liposomes with a composition of DOPC:DODAB 70:30 decorated with a different number of polyelectrolyte layers, N, of PSS/PAH and PSS/PDADMAC pairs.

Fig. 6 shows the reflective profiles obtained in SAXS experiments for liposomes decorated with a different number of layers. The results indicate that the adsorption of the first anionic PSS layer on the bare liposome leads to the emergence of a well-defined Bragg peak at a wavevector value around 1.1 nm^{-1}. This suggests homogeneous adsorption of the PSS layer onto the liposome surface, leading to a well-defined lamellar structure, which is compatible with the enhanced packing observed in ESR experiments upon the deposition of the first PSS layer. The thickness of the PSS layer can be obtained from the position of the diffraction peak according to $d = 2\pi/q$, presenting a value of 5.5 nm in this case. This thickness is in good agreement with the one obtained by DLS in our previous study [27].

The deposition of the polycation layer on the initially PSS-decorated liposomes leads to the disappearance of the Bragg peak, independently of the nature of the deposited polycation. This effect can be explained considering that the molecules of the deposited anionic PSS present strong electrostatic interactions with both the cationic molecules of the second layer and the DODAB molecules of the lipid membrane. This effect conducts to the weakening of the initial ionic cross-linking between the initially deposited layer, leading to a more disordered structure. This behaviour is more evident in the case of the deposition of PDADMAC layer (Fig. 6b), which can be explained considering their higher average molecular weight and polydispersity, leading to a more fuzzy structure. The deposition of the third layer (PSS) results again in the appearance of a Bragg peak in the scattering profile, at a wavevector corresponding to a characteristic length of 5.9 nm. The reappearance of this peak indicates that the PSS adsorption

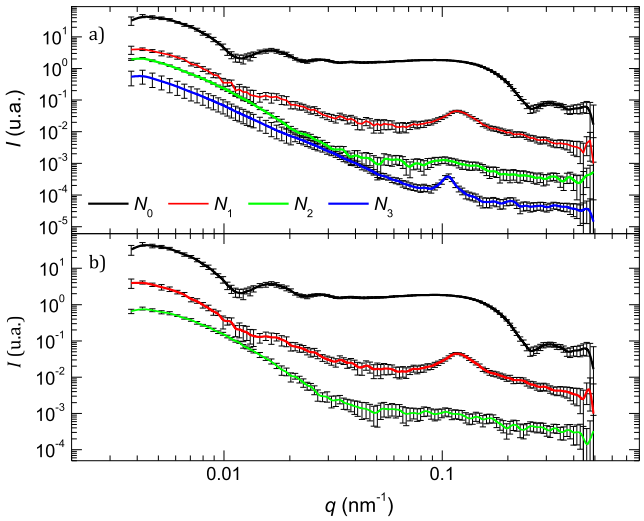

Fig. 6. SAXS scattering profiles for liposomes with composition 70:30 DOPC:DODAB and nominal diameter of 50 nm coated by a different number of polyelectrolyte layers (N_0: bare liposome, N_1: liposome + one polyelectrolyte layer, N_2: liposome + two polyelectrolyte layers and N_3: liposome + three polyelectrolyte layers). Multilayers with two different polyelectrolyte pairs were studied: a) PSS/PAH and b) PSS/PDADMAC. The solid lines correspond to the modelled reflectivity profiles.

induces the rearrangement of the lamellar structure, in agreement with the ESR results. Therefore, it can be assumed that the spherical lamellar structure of the system undergoes a contraction process upon the deposition of anionic layers and an expansion one once the cationic layers are deposited, as evidenced by the differences in the SAXS scattering profiles, i.e., the appearance-disappearance of the Bragg peak. This behaviour can be considered in good agreement with the above discussion on the dependence of the relaxation time with the layer deposition obtained from the ESR experiments, i.e., the emergence of an odd–even effect in the relaxation times, and the consequent rigidification-fluidification of the liposome membrane.

Moreover, the corresponding pair distributions, $p(r)$, obtained for each SAXS scattering profile depicted in Fig. 7 show that the deposition of polymer on the liposomes leads to a shifting of the position of the maximum to shorter distances, which is in good agreement with the contraction effect above mentioned. Furthermore, after the deposition of the polymer layers the pair distributions become broader. This, combined with the shifting of the position of the maximum, suggests that the deposition of the polyelectrolyte layers induces the deformation of the liposomes towards an ellipsoidal-limit, even though the results evidence that the curvature does not correspond to a true rod-like system [39]. This change in the morphology of the liposomes after coating agrees qualitatively with the results by Hassan et al. [50] for polyethylene glycol decorated vesicles. It should be noted that the width of the pair distribution shown in Fig. 7a suggests a certain degree of aggregation of the polyelectrolyte decorated liposomes, as was confirmed by the analysis of the SANS scattering profiles displayed in Fig. 8 for capsules decorated with both polyelectrolyte pairs.

The corresponding SANS curves of the bare liposomes present in the low q region a constant dependence of the scattered intensity with q^2. However, when the different polyelectrolyte layers are deposited, the scattered intensity increases, indicating long-range interactions between the capsules, which can lead to their partial aggregation in agreement with the results reported in our previous publication based in DLS experiments [27]. Despite this effect, in the high q region the profiles of SANS curves are very similar to

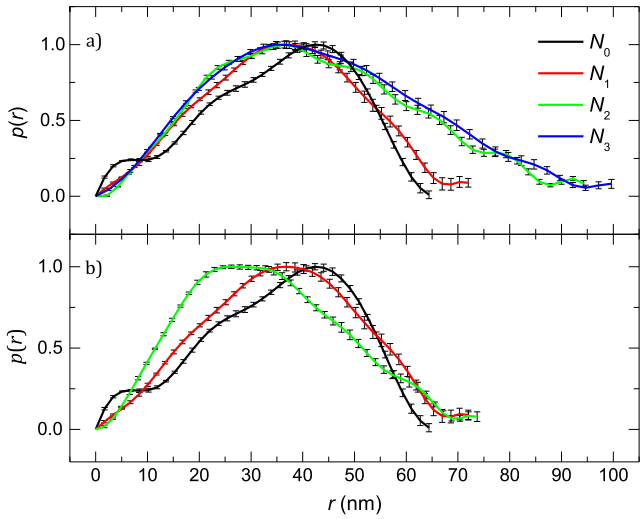

Fig. 7. Pair distributions, $p(r)$, obtained from the SAXS scattering profiles of liposomes with composition 70:30 DOPC:DODAB and nominal diameter of 50 nm coated by different number of polyelectrolyte layers (N_0: bare liposome, N_1: liposome + one polyelectrolyte layer, N_2: liposome + two polyelectrolyte layers and N_3: liposome + three polyelectrolyte layers). Multilayers of two different polyelectrolyte pairs were studied: a) PSS/PAH and b) PSS/PDADMAC.

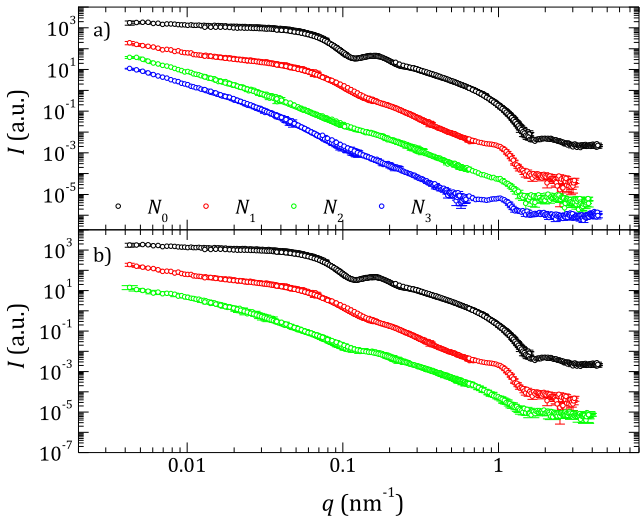

Fig. 8. SANS scattering profiles of liposomes with composition 70:30 DOPC:DODAB and nominal diameter of 50 nm coated by different number of polyelectrolyte layers (N_0: bare liposome, N_1: liposome + one polyelectrolyte layer, N_2: liposome + two polyelectrolyte layers and N_3: liposome + three polyelectrolyte layers). Multilayer of two different polyelectrolyte pairs were studied: a) PSS/PAH and b) PSS/PDADMAC.

those obtained in SAXS. Thus, the adsorption of the anionic layers leads also to the emergence of a Bragg diffraction peak, which disappears with the adsorption of the cationic one. This behaviour agrees with the formation of an ordered lamellar structure after the adsorption of PSS layers, which contrasts with the fuzzy character of the structure found after the deposition of PAH and PDADMAC layers. This fuzzier character of LbL capped with polycation layers was ascribed by Ghostine et al. [51] and Guzmán et al. [23,52]. to changes in the type of charge compensation mechanism of polycation and polyanion layers.

4. Conclusions

This work has explored the effect of the alternate deposition of polyelectrolyte layers bearing oppositely charges on the internal structure of polyelectrolyte-decorated liposomes, which plays a very important role in the control of important properties of these systems, e.g., porosity and permeability, for their application with encapsulation purposes [3,4]. The results have shown that the alternate deposition of oppositely charged polyelectrolytes on the external leaflet of positively charged liposomes allows modulating the organization of the fabricated supramolecular structures, impacting the packing and rigidity of the capsule. This results from the strength of the ionic cross-linking between adjacent layers [48], which is mostly determined by the specific charge of the last deposited layer, with an almost negligible role of the specific chemistry of the deposited polymer. However, the latter presents a very important impact on the fuzziness of the supramolecular system. Furthermore, the ability for modulating the packing and lamellar ordering of multi-layered film by the alternate deposition of polyelectrolyte bearing opposite charges presents a very important role in the control of the release profiles of encapsulated compounds due to its impact on the permeability of the LbL structure [13]. Thus, even though this study is limited to the deposition of a reduced number of layers, its results open interesting avenues for modulating the properties of polyelectrolyte capsules in such a way that they can be exploited for design suitable platforms for the encapsulation of different types of molecules.

In summary, the present work has contributed to deepening the current understanding about the organization of polyelectrolyte layers within LbL capsules [24–26], which was up to the dated an almost unexplored aspect towards a rational design of a new generation of drug delivery platforms based on the LbL technology.

Funding

This work was funded by MICINN (Spain) under grant PID2019-106557 GB-C21 and by E.U. on the framework of the European Innovative Training Network-Marie Sklodowska-Curie Action NanoPaInt (grant agreement 955612).

Data availability

Data will be made available on request.

Declaration of Competing Interest

The authors declare that they have no known competing financial interests or personal relationships that could have appeared to influence the work reported in this paper.

Acknowledgements

This work was funded by MICINN (Spain) under grant PID2019-106557 GB-C21 and by E.U. on the framework of the European Innovative Training Network-Marie Sklodowska-Curie Action NanoPaInt (grant agreement 955612). The CAI of Resonancia Magnética Nuclear y Espín Electrónico and the Centro de Espectroscopía y Correlación both belonging to the Universidad Complutense de Madrid are acknowledged for the use of their facilities. Authors also want to thank to the ILL for beamtime allocation of the proposal number 9-13-787 (doi: 10.5291/ILL-DATA.9-13-787).

Author contribution

E.G, R.G.R. and F.O. conceived and planned the experiments. A. M.M., J.E.F.R., A.M. and S.P. carried out the experiments. E.G. and A.M.M. performed data analysis. F.O., R.G.R., E.G, A.M.M., A.M.

and S.P. contributed to the interpretation of the results. A.M.M. and E.G. wrote the manuscript with input from all authors.

Appendix A. Supplementary material

Supplementary data to this article can be found online at https://doi.org/10.1016/j.jcis.2023.02.086.

References

[1] M. Delcea, H. Möhwald, A.G. Skirtach, Stimuli-responsive LbL capsules and nanoshells for drug delivery, Adv. Drug. Deliv. Rev. 63 (2011) 730–747.
[2] L.L. del Mercato, P. Rivera-Gil, A.Z. Abbasi, M. Ochs, C. Ganas, I. Zins, C. Sönnichsen, W.J. Parak, LbL multilayer capsules: recent progress and future outlook for their use in life sciences, Nanoscale 2 (2010) 458–467.
[3] L.L. del Mercato, M.M. Ferraro, F. Baldassarre, S. Mancarella, V. Greco, R. Rinaldi, S. Leporatti, Biological applications of LbL multilayer capsules: from drug delivery to sensing, Adv. Colloid Interface Sci. 207 (2014) 139–154.
[4] A. Mateos-Maroto, I. Abelenda-Núñez, F. Ortega, R.G. Rubio, E. Guzmán, Polyelectrolyte Multilayers on Soft Colloidal Nanosurfaces: A New Life for the Layer-By-Layer Method, Polymers 13 (2021) 1221.
[5] E. Guzmán, A. Mateos-Maroto, M. Ruano, F. Ortega, R.G. Rubio, Layer-by-Layer polyelectrolyte assemblies for encapsulation and release of active compounds, Adv. Colloid Interface Sci. 249 (2017) 290–307.
[6] A. Mateos-Maroto, L. Fernández-Peña, I. Abelenda-Núñez, F. Ortega, R.G. Rubio, E. Guzmán, Polyelectrolyte multilayered capsules as biomedical tools, Polymers 14 (2022) 479.
[7] E. Guzmán, R.G. Rubio, F. Ortega, A closer physico-chemical look to the Layer-by-Layer electrostatic self-assembly of polyelectrolyte multilayers, Adv. Colloid Interface Sci. 282 (2020) 102197.
[8] L. Xu, Z. Chu, H. Wang, L. Cai, Z. Tu, H. Liu, C. Zhu, H. Shi, D. Pan, J. Pan, X. Fei, Electrostatically assembled multilayered films of biopolymer enhanced nanocapsules for on-demand drug release, ACS Appl. Bio Mat- 2 (2019) 3429–3438.
[9] G. Nifontova, M. Zvaigzne, M. Baryshnikova, E. Korostylev, F. Ramos-Gomes, F. Alves, I. Nabiev, A. Sukhanova, Next-generation theranostic agents based on polyelectrolyte microcapsules encoded with semiconductor nanocrystals: development and functional characterization, Nanoscale Res. Lett. 13 (2018) 30.
[10] A.M. Pavlov, V. Saez, A. Cobley, J. Graves, G.B. Sukhorukov, T.J. Mason, Controlled protein release from microcapsules with composite shells using high frequency ultrasound—potential for in vivo medical use, Soft Matter 7 (2011) 4341–4347.
[11] L.I. Kazakova, L.I. Shabarchina, S. Anastasova, A.M. Pavlov, P. Vadgama, A.G. Skirtach, G.B. Sukhorukov, Chemosensors and biosensors based on polyelectrolyte microcapsules containing fluorescent dyes and enzymes, Anal. Bioanal. Chem. 405 (2013) 1559–1568.
[12] E.V. Musin, A.L. Kim, A.V. Dubrovskii, S.A. Tikhonenko, New sight at the organization of layers of multilayer polyelectrolyte microcapsules, Sci. Rep. 11 (2021) 14040.
[13] A.A. Antipov, G.B. Sukhorukov, S. Leporatti, I.L. Radtchenko, E. Donath, H. Möhwald, Polyelectrolyte multilayer capsule permeability control, Colloids Surf. A 198–200 (2002) 535–541.
[14] D.B. Trushina, T.V. Bukreeva, T.N. Borodina, D.D. Belova, S. Belyakov, M.N. Antipina, Heat-driven size reduction of biodegradable polyelectrolyte multilayer hollow capsules assembled on CaCO3 template, Colloids Surf. B 170 (2018) 312–321.
[15] J. Campbell, J. Abnett, G. Kastania, D. Volodkin, A.S. Vikulina, Which biopolymers are better for the fabrication of multilayer capsules? a comparative study using vaterite caco3 as templates, ACS Appl. Mat. Interfaces 13 (2021) 3259–3269.
[16] F. Kazemi-Andalib, M. Mohammadikish, A. Divsalar, U. Sahebi, Hollow microcapsule with pH-sensitive chitosan/polymer shell for in vitro delivery of curcumin and gemcitabine, Eur. Polym. J. (2021) 110887.
[17] K. Szczepanowicz, U. Bazylińska, J. Pietkiewicz, L. Szyk-Warszyńska, K.A. Wilk, P. Warszyński, Biocompatible long-sustained release oil-core polyelectrolyte nanocarriers: from controlling physical state and stability to biological impact, Adv. Colloid Interface Sci. 222 (2015) 678–691.
[18] A. Eivazi, B. Medronho, B. Lindman, M. Norgren, On the development of all-cellulose capsules by vesicle-templated layer-by-layer assembly, Polymers 13 (2021) 589.
[19] E. Guzmán, H. Ritacco, J.E.F. Rubio, R.G. Rubio, F. Ortega, Salt-induced changes in the growth of polyelectrolyte layers of poly(diallyl-dimethylammonium chloride) and poly(4-styrene sulfonate of sodium), Soft Matter 5 (2009) 2130–2142.
[20] E. Guzmán, H. Ritacco, F. Ortega, R.G. Rubio, Evidence of the influence of adsorption kinetics on the internal reorganization of polyelectrolyte multilayers, Colloids Surf. A 384 (2011) 274–281.
[21] M. Lösche, J. Schmitt, G. Decher, W.G. Bouwman, K. Kjaer, Detailed structure of molecularly thin polyelectrolyte multilayer films on solid substrates as revealed by neutron reflectometry, Macromolecules 31 (1998) 8893–8906.
[22] J. Schmitt, T. Gruenewald, G. Decher, P.S. Pershan, K. Kjaer, M. Loesche, Internal structure of layer-by-layer adsorbed polyelectrolyte films: a neutron and x-ray reflectivity study, Macromolecules 26 (1993) 7058–7063.
[23] E. Guzmán, A. Maestro, S. Llamas, J. Álvarez-Rodríguez, F. Ortega, Á. Maroto-Valiente, R.G. Rubio, 3D solid supported inter-polyelectrolyte complexes obtained by the alternate deposition of poly(diallyldimethylammonium chloride) and poly(sodium 4-styrenesulfonate), Beilstein J. Nanotechnol. 7 (2016) 197–208.
[24] I. Estrela-Lopis, S. Leporatti, D. Clemens, E. Donath, Polyelectrolyte multilayer hollow capsules studied by small-angle neutron scattering SANS, Soft Matter 5 (2009) 214–219.
[25] I. Estrela-Lopis, S. Leporatti, S. Moya, A. Brandt, E. Donath, H. Möhwald, SANS studies of polyelectrolyte multilayers on colloidal templates, Langmuir 18 (2002) 7861–7866.
[26] I. Estrela-Lopis, S. Leporatti, E. Typlt, D. Clemens, E. Donath, Small angle neutron scattering investigations (SANS) of polyelectrolyte multilayer capsules templated on human red blood cells, Langmuir 23 (13) (2007) 7209–7215.
[27] M. Ruano, A. Mateos-Maroto, F. Ortega, H. Ritacco, J.E.F. Rubio, E. Guzmán, R.G. Rubio, Fabrication of robust capsules by sequential assembly of polyelectrolytes onto charged liposomes, Langmuir 37 (2021) 6189–6200.
[28] S.G.M. Ong, M. Chitneni, K.S. Lee, L.C. Ming, K.H. Yuen, Evaluation of extrusion technique for nanosizing liposomes, Pharmaceutics 8 (4) (2016) 36.
[29] B.J. Berne, R. Pecora, Dynamic light scattering with applications to chemistry, biology, and Physics Dover Publications Inc, New York, 2000.
[30] L. Fernández-Peña, E. Guzmán, F. Ortega, L. Bureau, F. Leonforte, D. Velasco, R. G. Rubio, G.S. Luengo, Physico-chemical study of polymer mixtures formed by a polycation and a zwitterionic copolymer in aqueous solution and upon adsorption onto negatively charged surfaces, Polymer 217 (2021) 123442.
[31] R.J. Hunter, Zeta potential in colloid science: principles and applications, Academic Press, London, UK, 1998.
[32] S.-H. Chen, T.-L. Lin, Colloidal Solutions, in: D.L. Price, K. Sköld (Eds.), Methods in Experimental Physics, Academic Press, London, UK, 1987, pp. 489–543.
[33] P. Balgavý, M. Dubničková, N. Kučerka, M.A. Kiselev, S.P. Yaradaikin, D. Uhríková, Bilayer thickness and lipid interface area in unilamellar extruded 1,2-diacylphosphatidylcholine liposomes: a small-angle neutron scattering study, Biochim. Biophys. Acta 1512 (2001) 40–52.
[34] L. Cipelletti, V. Trappe, D.J. Pine, Scattering techniques, fluids, colloids and soft materials, John Wiley & Sons Inc, Hoboken, NJ, USA, 2016.
[35] B. Yue, C.-Y. Huang, M.-P. Nieh, C.J. Glinka, J. Katsaras, Highly stable phospholipid unilamellar vesicles from spontaneous vesiculation: a DLS and SANS study, J. Phys. Chem. B 109 (2005) 609–616.
[36] D. Lombardo, P. Calandra, M.A. Kiselev, Structural characterization of biomaterials by means of small angle X-rays and Neutron Scattering (SAXS and SANS), and light scattering experiments, Molecules 25 (2020) 5624.
[37] E. Di Cola, I. Grillo, S. Ristori, Small Angle X-ray and neutron scattering: powerful tools for studying the structure of drug-loaded liposomes, Pharmaceutics 8 (2016) 10.
[38] M.B. Frampton, D. Marquardt, I. Letofsky-Papst, G. Pabst, P.M. Zelisko, Analysis of Trisiloxane Phosphocholine Bilayers, Langmuir 33 (2017) 4948–4953.
[39] D.I. Svergun, M.H.J. Koch, Small-angle scattering studies of biological macromolecules in solution, Rep. Prog. Phys. 66 (10) (2003) 1735–1782.
[40] L. Ding, E.Y. Chi, K.S. Schanze, G.P. Lopez, D.G. Whitten, Insight into the mechanism of antimicrobial conjugated polyelectrolytes: lipid headgroup charge and membrane fluidity effects, Langmuir 26 (2010) 5544–5550.
[41] J.B. de la Serna, G. Orädd, L.A. Bagatolli, A.C. Simonsen, D. Marsh, G. Lindblom, J. Perez-Gil, Segregated phases in pulmonary surfactant membranes do not show coexistence of lipid populations with differentiated dynamic properties, Biophysical. J. 97 (2009) 1381–1389.
[42] R. Guzzi, R. Bartucci, Electron spin resonance of spin-labeled lipid assemblies and proteins, Archiv. Biochm Biophys. 580 (2015) 102–111.
[43] E. Feitosa, P.C.A. Barreleiro, G. Olofsson, Phase transition in dioctadecyldimethylammonium bromide and chloride vesicles prepared by different methods, Chem.Phys. Lipids 105 (2) (2000) 201–213.
[44] J.R. Silvius, Thermotropic phase transitions of pure lipids in model membranes and their modifications by membrane proteins, Lipid-protein interactions 2 (1982) 239–281.
[45] A. Cruz, D. Marsh, J. Pérez-Gil, Rotational dynamics of spin-labelled surfactant-associated proteins SP-B and SP-C in dipalmitoylphosphatidylcholine and dipalmitoylphosphatidylglycerol bilayers, Biochimica et Biophysica Acta (BBA) -, Biomembranes 1415 (1) (1998) 125–134.
[46] F.-G. Wu, Z.-W. Yu, G. Ji, Formation and transformation of the subgel phase in dioctadecyldimethylammonium bromide aqueous dispersions, Langmuir 27 (2011) 2349–2356.
[47] J. Filipovic-Grcic, N. Skalko-Basnet, I. Jalsenjak, Mucoadhesive chitosan-coated liposomes: characteristics and stability, J. Microencapsul. 18 (2001) 3–12.
[48] A.M. Lehaf, H.H. Hariri, J.B. Schlenoff, Homogeneity, modulus, and viscoelasticity of polyelectrolyte multilayers by nanoindentation: refining the buildup mechanism, Langmuir 28 (2012) 6348–6355.
[49] G. Angelini, M. Chiarini, P. De Maria, A. Fontana, C. Gasbarri, G. Siani, D. Velluto, Characterization of cationic liposomes. influence of the bilayer composition on the kinetics of the liposome breakdown, Chem. Phys. Lipids. 164 (2011) 680–687.
[50] B. Dutta, K.C. Barick, G. Verma, V.K. Aswal, I. Freilich, D. Danino, B.G. Singh, K.I. Priyadarsini, P.A. Hassan, PEG coated vesicles from mixtures of Pluronic P123

and l-α-phosphatidylcholine: structure, rheology and curcumin encapsulation, Phys. Chem. Chem. Phys. 19 (2017) 26821–26832.
[51] R.A. Ghostine, M.Z. Markarian, J.B. Schlenoff, Asymmetric growth in polyelectrolyte multilayers, J. Am. Chem. Soc. 135 (2013) 7636–7646.
[52] E. Guzmán, F. Ortega, R.G. Rubio, Comment on "Formation of polyelectrolyte multilayers: ionic strengths and growth regimes" by K. Tang and A. M. Besseling, Soft Matter 12, 1032, Soft Matter 12 (2016) 8460–8463.